RAPID COMMUNICATIONS

PHYSICAL REVIEW B VOLUME 35, NUMBER 14 15 MAY 1987-I

Light-induced defect creation in hydrogenated amorphous silicon: A detailed examination using junction-capacitance methods

K. K. Mahavadi, K. Zellama,* and J. D. Cohen
University of Oregon, Eugene, Oregon 97403

J. P. Harbison
Bell Communication Research, Murray Hill, New Jersey 07974
(Received 27 February 1987)

From junction-capacitance measurements we have determined the density, energy distribution, and electronic occupation of light-induced metastable defects near the midgap for a set of nearly intrinsic hydrogenated-amorphous-silicon samples with well-characterized impurity levels. In particular, we have inferred the changes in both neutral and negative dangling bonds for a series of isochronal anneals between the light-soaked state and full-dark-annealed state of each sample. Our results indicate that the dominant defect-creation mechanism is *not* Si—Si bond breaking, and also indicate the existence of at least two quasi-independent metastable defect-creation processes.

A key element in the Staebler-Wronski effect in hydrogenated amorphous silicon (a-Si:H) is the light-induced increase in the midgap dangling-bond (DB) density of states. However, there is considerable disagreement about the fundamental mechanisms of such defect creation. A popular current model, proposed on the basis of electron-spin-resonance (ESR) studies,[1,2] is that recombination of photoinduced carriers can break weak Si—Si bonds. However, recent optical absorption studies[3] and other ESR studies[4] seem to disagree with some of the detailed aspects of that model. In this Rapid Communication, we describe extensive new studies of the metastable defect creation using junction-capacitance methods on undoped amorphous silicon films. Because capacitance measurements disclose the absolute number of occupied gap states regardless of spin, such information allows us to examine new aspects of the defect-creation models that have been proposed. And while capacitance methods have been applied to this problem previously,[5-7] this is the first study to map out the energy and spatial dependence of the metastable defects near midgap as a function of light saturation and partial annealing.

One lightly PH_3-doped and five nominally undoped samples were grown by the glow-discharge method on p^+ crystalline silicon at substrate temperatures of $255 \pm 5\,°C$. The SiH_4-to-Ar gas ratios are given in Table I. Semitransparent Schottky barriers of Pd were used for the top contact; however, the measurements reported below use an applied bias which depletes the p^+ substrate barrier junction. Secondary-ion mass spectroscopy (SIMS) results[8] for oxygen, nitrogen, carbon, and phosphorous impurities are summarized in Table I. These concentrations are listed over the region where we believe the capacitance measurements actually probe each sample.

Samples were prepared in a light-saturated state (state B) by exposure to 1.9-eV light from a cw krypton laser at 400 mW/cm^2 (corrected for the semitransparent metal contact) at room temperature for 2.5 h. Samples were annealed isochronally at 10- or 20-K temperature intervals, beginning with a 5-min anneal at 380 K, up to a temperature of 473 K (state A). Capacitance versus temperature (C-T) measurements were carried out over the range 250–400 K at frequencies from 2 Hz to 1 kHz for every metastable "state" of each sample studied. As discussed

TABLE I. Sample characteristics comparing the impurity concentrations determined by SIMS analysis with the deep defect densities determined by drive-level capacitance measurements in state-A and the light-saturated state-$B1$ (following a 380-K anneal). The Fermi-level positions as determined by the analysis of the drive-level measurements are also given.

Sample	SiH_4-Ar ratio (%)	SIMS-determined impurity concentrations: phosphorous (cm^{-3})	oxygen (cm^{-3})	nitrogen (cm^{-3})	carbon (cm^{-3})	Fermi-level position: state A (eV)	state $B1$ (eV)	Deep defect density: state A (cm^{-3})	state $B1$ (cm^{-3})
1	50	2×10^{18}	4×10^{19}	1×10^{18}	3.5×10^{18}	0.50	0.59	2.4×10^{16}	5.3×10^{16}
2	30	7×10^{16}	2×10^{19}	4×10^{18} [a]	3×10^{18}	0.69	0.65	3.1×10^{16}	7.2×10^{16}
3	100	8×10^{16}	2.5×10^{19}	1.5×10^{19} [a]	2.5×10^{18} [a]	0.62	0.66	2.4×10^{16}	4.3×10^{16}
4	30	1×10^{17} [a]	3×10^{19}	2.5×10^{18}	7×10^{18} [a]	0.68	0.60	4.9×10^{15}	1.7×10^{16}
5	10	2×10^{16}	1.5×10^{19}	1.5×10^{18}	3×10^{18}	0.58	0.66	3.5×10^{15}	8.6×10^{15}
6	100	6×10^{16}	2×10^{19}	2×10^{18}	1.4×10^{19} [a]	0.64	0.73	4.4×10^{15}	3.6×10^{16}

[a]SIMS analysis indicated a spatial variation for this impurity in excess of a factor of 1.5 μm^{-1}.

 © 1987 The American Physical Society

previously,[5] such data allow us to obtain the activation energy of the conductivity, E_σ, and the value of $g(E_F)$ for each partial-anneal state. This determination of E_σ is considered more reliable than coplanar measurements because it is unaffected by surface barrier potentials and thus is more likely to reflect bulk film transport properties.

The primary method we employ is called "drive-level (DL) capacitance profiling" and has been described in detail elsewhere.[9] This technique experimentally determines the gap-state occupation

$$N_{\rm DL}=\int_{E_c-E_e}^{E_F^0} g(E)dE\ , \tag{1}$$

where E_F^0 is the Fermi-level position in the bulk sample and the lower-energy cutoff E_e is given by the relation $E_e(\omega,T)=k_BT\ln(\nu/\omega)$. Here ω is the (angular) ac measurement frequency and ν lies in the range 10^{12}–10^{13} sec^{-1}. The spatial dependence of $N_{\rm DL}$ is obtained by varying the applied dc bias to the junction as in standard profiling measurements. The *energy* dependence of the density of states may be examined by increasing the temperature to increase the range of integration in Eq. (1).

Typical results from 100-Hz drive-level profiling measurements are shown for sample 6 in Fig. 1(a). Each data point for each anneal state represents the spatially averaged value of $N_{\rm DL}$ taken over a 0.1–0.2-μm range near one spatial region for each sample. On the top scale, the measurement temperatures are indicated; on the bottom scale, we have converted this temperature into an energy depth E_e using $\nu=1\times10^{13}$ sec^{-1}. Each curve therefore represents the value of the integral in Eq. (1) plotted as a function of E_e.

The derivative with respect to energy of the curves in Fig. 1(a) will yield the density of states. Because of the limited energy range of these data (typically 100–150 meV) we generally obtain only the average value of $g(E)$ and an indication of its slope in the vicinity of E_e below E_c. However, taken together with the value of $g(E_F)$ determined by *C-T* measurements one can infer a peaked distribution for $g(E)$ with a maximum near the middle of the gap. We have thus parametrized $g(E)$ in this energy range by a Gaussian defect band characterized by its energy position, energy width, and magnitude, which are fit from the values of $g(E_F)$, $g(E_c-E_e)$, and $g'(E_c-E_e)$ determined above. Such fits were further constrained by requiring a smooth monotonic variation of parameters between partial-anneal states. One additional piece of information came from the absolute magnitude of $N_{\rm DL}$ (apart from its derivatives). This may be used to infer a value of E_F^0 independent of the measured value of E_σ. Using this method we hoped to avoid potential ambiguities associated with E_σ due to statistical shifts or the Meyer-Neldel rule. These values of E_F^0 were, in most cases, 100 to 150 meV shallower than the corresponding E_σ values.

The deduced $g(E)$ and values of E_F^0 for sample 6 are shown in Fig. 1(b). These results are in good qualitative agreement with many other measurements which indicate a metastable increase in DB density and a monotonic shift of E_F toward midgap with increasing light exposure. Small changes in the peak positions or widths in this sample are *not* significant within experimental error.

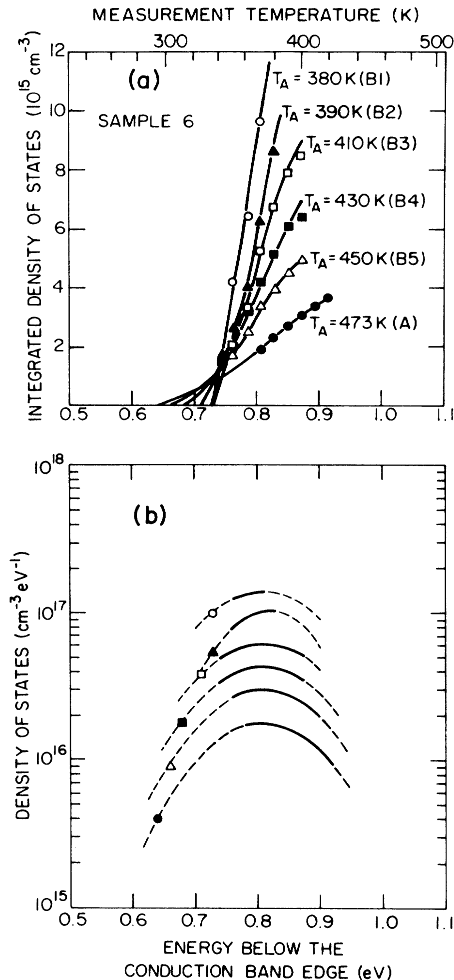

FIG. 1. (a) Drive-level densities for sample 6 as a function of temperature for state *A* plus five partial anneal "states" produced by anneal temperatures, T_A, as indicated. The solid lines drawn through the data points are obtained by integrating the densities of states shown in (b). (b) Densities of states deduced by sample 6 from the data in (a). The solid line portion of each curve indicates the energy range of the drive-level data. The single data point at low energy for each curve is the value of $g(E_F)$ deduced from the *C-T* measurements.

A second example of such data is displayed for sample 2 in Fig. 2. The overall behavior for this sample is similar to that above; however, the shift in the peak position of the Gaussian defect band appears to be experimentally significant. This shift implies that the metastable defect band lies roughly 0.1 eV closer to the conduction band than the intrinsic DB band. Indeed, for anneal states near state *A* the distribution does not seem to match a single Gaussian band. Note also that E_F in this sample moves toward *deeper* energies in the final high-temperature anneal. Although unexplained at present, this anomalous shift is exactly mirrored in the dark conductivity behavior in this sample.

Data of this kind displayed in Figs. 1(a) and 2(a) provide very detailed information about metastable defect

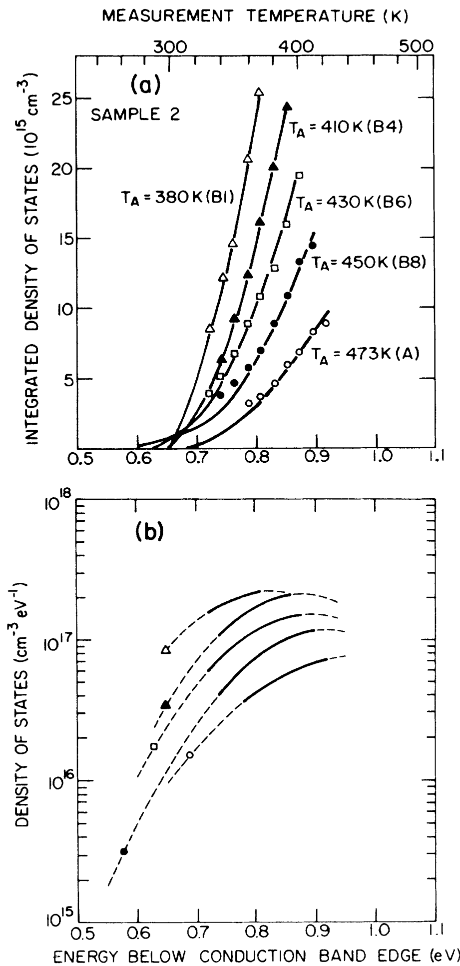

FIG. 2. Summary of drive-level densities and derived densities of states for sample 2 in state A and series of metastable states. Other details concerning the displayed curves are as in Fig. 1.

creation. In particular, if the defects probed in this energy range belong to the dangling-bond D^- subband as indicated by a variety of ESR studies,[1,10] then these data are totally inconsistent with the Si bond-breaking model. is, to preserve the total number of electrons, that model requires that the shaded regions of occupied states in Fig. 3(a) must remain fixed. Because the drive-level measurements give precisely the integral from E_F^0 down to an energy E_e below E_c [see Eq. (1)], we would predict the drive-level values to become equal when E_e reaches E_M at roughly 0.9 to 1.0 eV below E_c. For values of E_e smaller than $E_c - E_M$, the value of N_{DL} should actually be smaller in state B than in state A due to the deeper Fermi level and hence smaller range of the integral for N_{DL} in state B [see Fig. 3(b)]. However, *all* the data show precisely the opposite behavior. This argues very strongly against a dominant role for the Si bond-breaking mechanism. Note that this argument applies independent of any Fermi level motion and, for symmetric D^0 and D^- subbands, is even independent of the degree of overlap of the DB defect subbands.

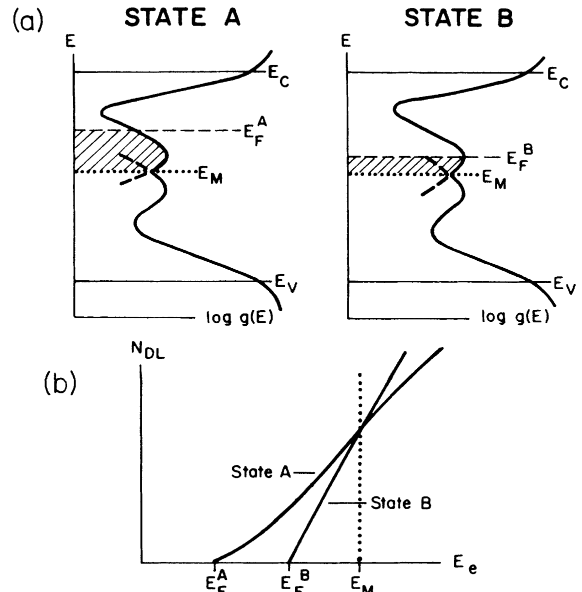

FIG. 3. (a) Schematic of the occupation of gap states in states A and B. In the Si—Si bond-breaking model the shaded regions must be equal. E_M labels the midpoint between the D^- and D^0 subbands. (b) General behavior of the drive-level density vs temperature predicted by the Si—Si bond-breaking model.

We may also estimate the changes in *both* the D^- and D^0 concentrations by integrating over energy the occupied and unoccupied portions, respectively, of the D^- bands displayed in Figs. 1(b) and 2(b). Such results are displayed in Fig. 4. We believe that the dissimilarity indi-

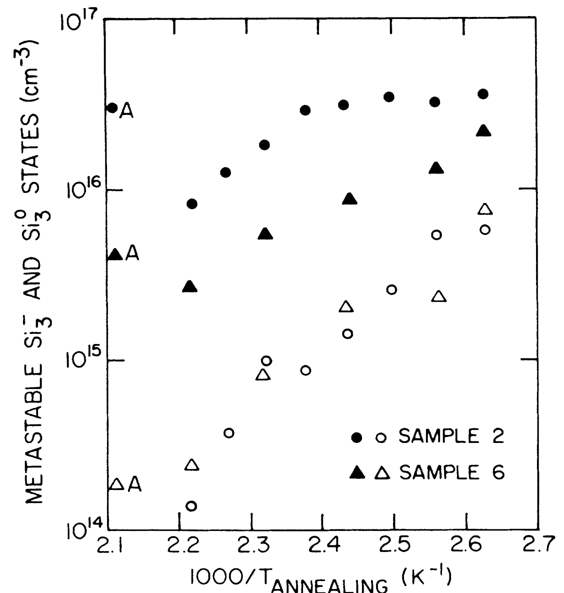

FIG. 4. Deduced metastable D^0 (open symbols) and D^- (filled symbols) defect densities for samples 2 and 5 as a function of anneal temperature. The state-A densities are also indicated. (For sample 2, the state-A density of D^0 centers is estimated to be negligible.)

cated between the annealing of D^0 and D^- metastable centers clearly indicates the existence of two quasi-independent processes. The suggestion of more than a single process in the light-induced effects in *a*-Si:H was made a few years ago on the basis of field-effect measurements.[11] It is, however, interesting to note that annealing behavior of the D^0 states is quite similar for all films. This is generally in agreement with the ESR studies which indicate metastable behavior independent of the impurity content[2] and also with the activation energy (of roughly 0.8 eV) observed for annealing metastable spins.[4]

Table I summarizes the Fermi-level shifts and deep-level defect densities for states A and $B1$ (the 380-K anneal state). These data indicate that the metastable defect increase is roughly comparable with the state-A defect density (except for sample 6), in general agreement with optical-absorption studies.[3] Also note that while samples 4, 5, and 6 have comparably low defect densities in state A, the metastable defect density of these samples varies by a factor of 6, roughly in proportion to their carbon content. This strongly suggests a carbon-related *extrinsic* component to the metastable behavior of these samples at carbon impurity levels of 100 ppm.

Because the dominant component of the metastable defect increase in our samples involves D^- centers, a defect-creation mechanism different than Si—Si bond breaking clearly must be found to account for these data. One possibility is a model (such as the one proposed by Adler[12]) in which local rearrangement of the atoms in the vicinity of DB's cause shifts of the associated energy levels within the mobility gap. Another possible mechanism concerns the roughly 1 ppm phosphorous contamination of our films. Robertson[13] has observed that the reaction $2Si_3{}^0+P_3{}^0 \rightarrow Si_3{}^- + P_4{}^+ + Si_4{}^0$ is exothermic. This implies that the reaction $Si_4{}^0+P_3{}^0 \rightarrow Si_3{}^- + P_4{}^+$ will be energetically more favorable than Si—Si bond breaking alone. The phosphorous content of the six films used in this study does not completely preclude such a mechanism. However, preliminary results on two totally phosphorous-free films indicate *no qualitative difference* in behavior from the above samples. Further experiments are now planned to examine the role of the other impurities in the observed D^- creation.

We gratefully acknowledge useful discussions with J. Robertson and M. Stutzmann. Work at the University of Oregon was supported in part by Solar Energy Institute Subcontracts No. XB-4-03101-1 and No. XB-6-06024-1.

*Current address: Université Paris VII, 75521 Paris Cédex 05, France.

[1] H. Dersch, J. Stuke, and J. Beichler, Appl. Phys. Lett. **38**, 456 (1981).

[2] M. Stutzmann, W. B. Jackson, and C. C. Tsai, Phys. Rev. B **32**, 23 (1985).

[3] A. Skumanich, N. Amer, and W. B. Jackson, Phys. Rev. B **31**, 2263 (1985).

[4] C. Lee, W. D. Ohlsen, P. C. Taylor, H. S. Ullal, and G. P. Ceasar, Phys. Rev. B **31**, 100 (1985).

[5] K. Zellama, J. D. Cohen, and J. P. Harbison, Mater. Res. Soc. Symp. Proc. **49**, 311 (1985).

[6] J. D. Cohen, D. V. Lang, J. P. Harbison, and A. M. Sergent, Solar Cells **9**, 119 (1983).

[7] A. Glade, J. Beichler, and H. Mell, J. Non-Cryst. Solids **77 & 78**, 397 (1985).

[8] SIMS analysis performed by Charles Evans and Associates, San Mateo, CA.

[9] C. E. Michelson, A. V. Gelatos, and J. D. Cohen, Appl. Phys. Lett. **47**, 412 (1985).

[10] J. D. Cohen, J. P. Harbison, and K. W. Wecht, Phys. Rev. Lett. **48**, 109 (1982).

[11] D. Han and H. Fritzsche, J. Non-Cryst. Solids **59 & 60**, 397 (1983).

[12] D. Adler, Solar Cells **9**, 133 (1983).

[13] J. Robertson, Phys. Rev. B **31**, 3817 (1985).